ELSEVIER

Journal of Alloys and Compounds 293–295 (1999) 788–794

Journal of ALLOYS AND COMPOUNDS

Effect of state of charge on impedance spectrum of sealed Ni–MH cells

Xianyou Wang[a,*], Bing Liu[b], Jie Yan[b], Huatang Yuan[b], Deying Song[b], Yunshi Zhang[b]

[a]*School of Chemistry and Chemical Engineering, Xiangtan University, Hunan 411105, China*
[b]*Institute of New Energy Material Chemistry, Nankai University, Tianjin 300071, China*

Abstract

Alternating current impedance spectroscopy was used to determine the state of charge of sealed Ni–MH cells in wide frequency range. A modified Randles' circuit was used to fit the impedance data. The effect of state of charge on the equivalent circuit parameters, e.g., phase angle, ϕ, impedance modulus, $|Z|$, equivalent series capacitance, C_s, ohmic resistance R_Ω and charge transfer resistance R_r was determined. It has been found that the impedance parameters were sensitive to state of charge at low frequencies.

Keywords: Ni–MH battery; Alternating current impedance spectroscopy; Equivalent circuit parameters

1. Introduction

The Ni–MH cell, which contains no toxic material and has a higher energy density and almost the same voltage as the conventional Cd–Ni cells, has become an important subject in the studies of power sources. Currently, Ni–MH cells are widely used as power sources for computer memory back-ups, portable videos, emergency lighting, electric vehicle and other important applications.

The state of charge of a cell refers to the ratio of residual capacity at a given instant to the maximum capacity available from the cell [1]. Knowledge of the state of charge not only helps indicating the residual capacity, but also helps in increasing the life expectancy of the cell by proper utilization. Many attempts have been made to determine the state of charge of a cell. Alternating current impedance technology is one of the important methods for nondestructive determination of the state of charge of a cell. Several investigators have used impedance technology to study the state of charge and conditions of Cd–Ni cells [2–7]. Barton et al. [4] found that the charge transfer resistance R_r decreased with increase in state of charge, while the double layer capacitance, C_{dl}, increased with increase in charge of state. Suresh and Sathyanarayana [5] measured the impedance of sealed Cd–Ni cells at low states of charge and found that at low charge states, the impedance of the nickel electrode dominated the cell impedance. Blanchard [6] determined the effect of state of charge on the R_r, C_{dl}, R_Ω and low frequency phase angle, ϕ. Sathyanarayana et al. [7] determined the effect of state of charge on phase angle, ϕ, C_s and C_p. There are few reports about the effect of state of charge on impedance spectrum of sealed Ni–MH cells. In present paper, an attempt will be made to account for the effect of state of charge on impedance spectrum of sealed Ni–MH cells.

2. Experimental

The Ni–MH cell tested was 1200 mAh AA type cell. The active material of positive electrode in the Ni–MH cell was the spherical nickel hydroxide that deposited 5% cobalt. The metal hydride (MH) electrode was $Mm(NiCoMnAl)_5$ storage hydrogen alloy powder. The cell was activated by charge–discharge cycles prior to impedance measurement. Charge was initially carried out at the C/5 rate for 6 h, resting for 30 min and discharge at the C/5 rate to the cut-off voltage of 1 V, where C is the nominal capacity of the cell. After a few cycles, impedance measurements were performed on the cell at various states of charge (SOC) as described below, with the measurements starting at 0% SOC.

The cell was discharged at C/5 rate to 1 V cut-off and impedance measurements were done at 0% SOC after the cell was on open circuit for 20 h. The cell was charged at C/5 rate for 1 h and impedance spectrum obtained after 20 h on open circuit. The cell was discharged at C/5 rate to 1

*Corresponding author.

0925-8388/99/$ – see front matter
PII: S0925-8388(99)00464-8

V after obtaining the spectrum to determine their actual state of charge. The cell was then charged at C/5 rate for 2 h. After 20 h on open circuit, the cell impedance spectrum was obtained. The cell was discharged at C/5 rate to 1 V and charged at C/5 rate for 3 h. This was repeated until impedance data was obtained at 100% SOC.

The impedance measurement was performed using 1287 electrochemical interface and 1250 frequency–response analyser. The EQUIV software developed by Boukamp [8] was used to fit the experimental data to the circuit and analyze the circuit parameters.

3. Results and discussion

Fig. 1a–f show the Nyquist plots for Ni–MH cell at various states of charge. It is interesting to note that the Nyquist plot at 0% state of charge consists of a smaller depressed semicircle and a line corresponding to the Warburg impedance; while impedance spectrum at other states of charge consist of two depressed semicircles at high and midfrequency and a line with 45°C towards the real axis at low frequency region. From the analysis of characteristics of Nyquist plots at various states of charge,

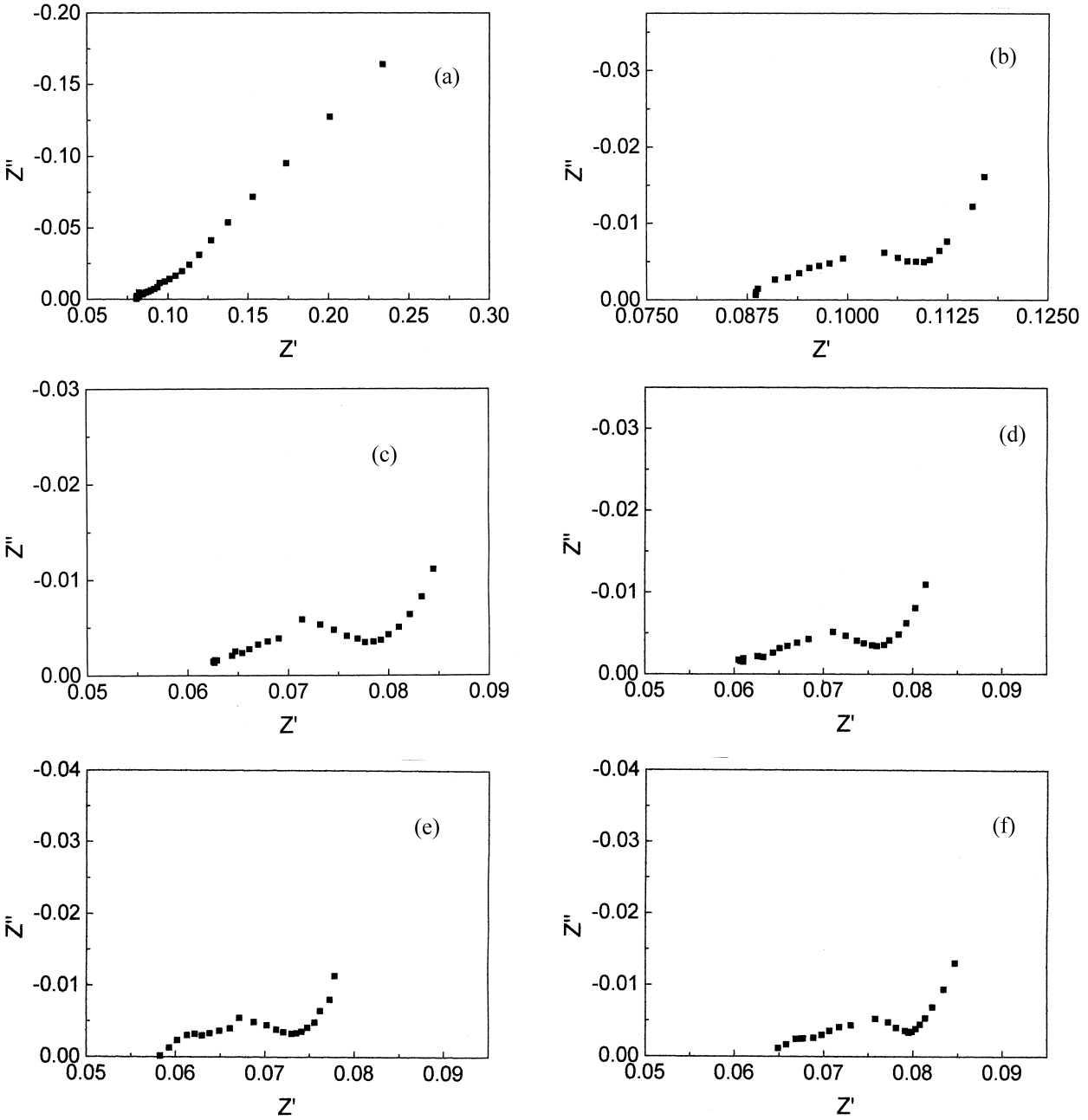

Fig. 1. Nyquist plots for Ni–MH cell at various states of charge (a) 0%, (b) 20%, (c) 40%, (d) 60%, (e) 80%, (f) 100%.

it seems that each plot contains a finite length diffusion element except at 0% SOC. The impedance of sealed Ni–MH cell is composed of contributions from the nickel hydroxide positive electrode, MH negative electrode, and the interelectrode region. Surech [9] has found that the impedance of sealed Cd–Ni cell at low state of charge is practically due to the nickel hydroxide electrode. Although Kuriyama et al. [11] measured impedance of electrodes made from an alloy powder ($MmNi_{3.5}Co_{0.7}Al_{0.8}$), very little data are available in the literature as yet on the impedance of hydride electrodes and Ni–MH cells. The Nyquist plot in Fig. 1a is apparently different from others in Fig. 1. The reasons for this are perhaps because the behavior of impedance of the cell at 0% state of charge is dominated mainly by nickel hydroxide, while for other states of charge the impedance of the metal hydride electrode is not negligible because a discharged nickel oxide electrode contains mainly nickel hydroxide, $Ni(OH)_2$, which is a poor electronic conductor. Reid [10] considered that the impedance of the sealed Ni–MH cell is probably due to the nickel electrode with the large portion. This conclusion is agreement with our measurements.

The imaginary components of the impedance at various states of charge at fixed frequencies are presented in Table 1. (Since the ohmic resistance forms a substantial portion of the real component of impedance, it masks the real component of the electrode impedance. Hence only the imaginary component has been presented.) The imaginary component of the impedance (Z'') goes through a minimum in the frequency range tested. Hence the state of charge cannot be determined from the value of the imaginary component at a fixed frequency. Sathyanarayana et al. [7] proposed to study the effect of state of charge on the characteristics of the cell by determining phase angle ϕ and equivalent series capacitance C_s, where C_s is the equivalent series capacitance of the cell. Since impedance of cell is very sensitive to state of charge at low frequencies and the inductive and capacitive components of the cell could not be separated, this paper mainly discusses the impedance characteristics at frequency as low as 0.01 Hz.

Table 1
Effect of state of charge on imaginary component (Z'') at various frequencies

SOC	Imaginary component Z'' (Ω)				
(%)	0.01 Hz	0.03981 Hz	0.1 Hz	0.25119 Hz	1 Hz
0	0.16406	0.07179	0.04122	0.02426	0.01472
20	0.01614	0.00766	0.00525	0.00501	0.00619
40	0.01115	0.00507	0.0037	0.00346	0.00477
60	0.01099	0.00487	0.00357	0.00353	0.0047
80	0.01137	0.00488	0.00358	0.00327	0.00447
100	0.01309	0.0054	0.00391	0.00341	0.00403

The cell impedance can be represented either as a series circuit R_sC_s or as a parallel resistance, respectively.

In impedance studies, the total impedance, Z, is usually the parameter that is measured between the two terminals of a cell. From the standard circuit theory, it can be given by [3]

$$Z = R_s - j/(\omega C_s) = (R_s\omega C_s - j)/(\omega C_s) \quad (1)$$

$$\frac{1}{Z} = \frac{\omega C_s(R_sC_s + j)}{(R_s\omega C_s - j)(R_s\omega C_s + j)} \quad (2)$$

$$= \frac{R_s\omega^2 C_s}{1 + (R_s\omega C_s)^2} + \frac{j\omega C_s}{1 + (R_s\omega C_s)^2} \quad (3)$$

where $j = \sqrt{-1}$; $\omega = 2\pi f$, f being the frequency (Hz).

Fig. 2a and b show the change of impedance modulus, $|Z|$, and phase angle, ϕ, with state of charge, respectively. Fig. 3 shows the change of equivalent series capacitance C_s with state of charge. Due to the greater sensitivity of the data with respect to frequency at various state of charge, for the sake of clearness, Fig. 3a and b show the relationship of C_s with state of charge at frequencies 0.01~0.25 Hz and 1~25 Hz, respectively. It is apparent from Fig. 2 that the curves a and b exhibited an initial decline, the lower the frequency was, the clearer initial decline was; moreover, the curves of changes of impedance modulus $|Z|$, and phase angle, ϕ, with state of charge all had a minimum. At low frequencies the change of $|Z|$ and ϕ with

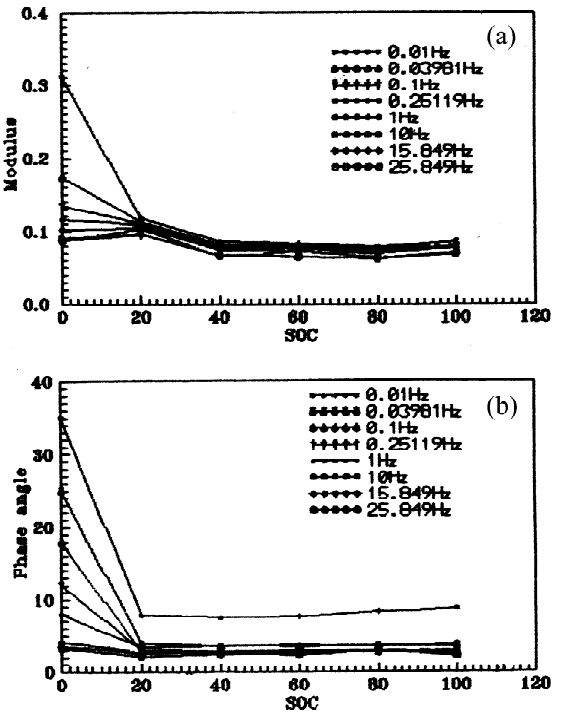

Fig. 2. Effect of state of charge on (a) impedance modulus, (b) impedance phase angle.

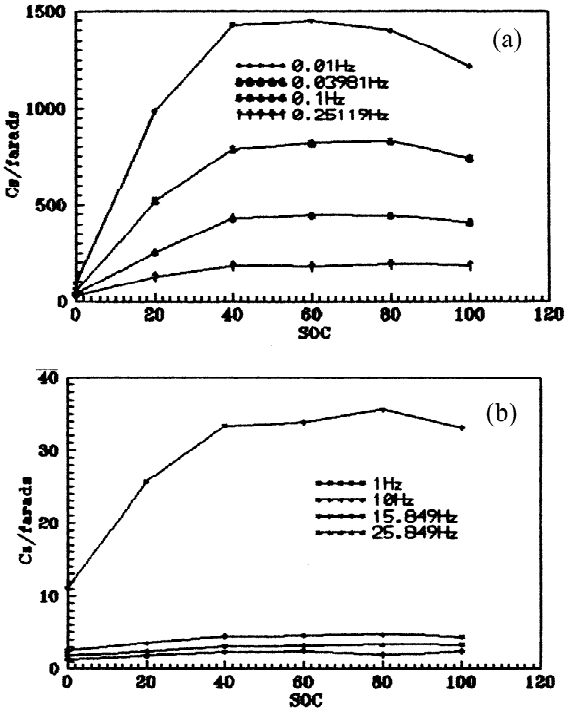

Fig. 3. Effect of state of charge on equivalent series capacitance C_s. (a) frequencies 0.01~0.25119 Hz. (b) frequencies 1~25.119 Hz.

state of charge were more obvious, especially at frequency 0.01 Hz. When the frequencies were greater than 10 Hz, the changes of $|Z|$ and ϕ with state of charge were very small. It can also been seen from Fig. 3 that when frequencies were below 10 Hz, the equivalent series capacitance C_s markedly changed with the change of state of charge. The lower the frequency was, the more marked this change became.

Although extensive literature has reported the state of charge of a cell at a fixed frequency, it is clear that such an approach may not always be successful. Seen from Figs. 2 and 3, at certain frequencies, the parameters, $|Z|$, ϕ and C_s pass through a maximum or minimum, thus making it difficult to determine the state of charge of the cell. However, it is clearly found that the above parameters increase or decrease with change of state of charge at lower frequencies, thus enabling determination of state of charge. Therefore, for Ni–MH cell, it can determine the state of charge by measurement of the above parameters at lower frequencies.

In Fig. 1, the Nyquist plot in each state of charge consists of two semicircles and a line except 0% state of charge. Thus, we use the modified Randles' circuit (Fig. 4) $R_\Omega(Q_1R_1)(Q_2(R_2Q_3))$, $R_\Omega(Q_1(R_1(Q_2(R_2Q_3))))$ and $R_\Omega(Q_1(R_1Q_3(Q_2R_2)))$ to fit experimental data, respectively. Where R_Ω is the ohmic resistance, R_1 and R_2 represent the charge transfer resistance, Q_1 and Q_2 are the constant phase elements representing double layer capacitance, and Q_3 is the constant phase element corresponding to the Warburg element. The impedance of a cell will have a contribution from charge- and mass-transfer processes as well as from the double-layer capacitance and inductance. The electrolyte solution and separator will contribute resistance to the cell impedance. Taking into account the above facts and by choosing a sufficiently low a.c. frequency for impedance measurements, it is possible to ensure that the inductive reactance is small compared to the capactive reactance so that neglecting the inductance reactance in the equivalent circuits shown in Fig. 4. Through treatment of data, we find that the circuit $R_\Omega(Q_1(R_1Q_3(Q_2R_2)))$ can fit satisfactorily experimental data. Fig. 5 shows the experimental and fitted Nyquist plots for Ni–MH cell at 80% state of charge. It can be clearly seen from Fig. 5 that the data was fitted with the modified Randles' circuit. Table 2 gives the values of the equivalent circuit parameters at various state of charge. According to the results in Table 2, it can determine the variation of ohmic resistance, R_Ω, and charge transfer resistance, R_r, with state of charge. The results are shown in Figs. 6 and 7, respectively. It can be found from Fig. 6 that the ohmic resistance decreased quickly with increase in 0~40% SOC and then changed slightly. The reasons for this phenomenon are due to no net generation or removal of OH^- ions during the charge–discharge reactions in Ni–MH cell, the electrolyte does not participate significantly and, moreover, the ohmic resistance of a sealed cell corresponds to the sum of the resistance of the electrolyte in the pores of the electrode and the separator but the electrode matrix also makes a contribution. Besides, the impedance of Ni–MH cell at low state of charge is dominated by nickel oxide electrode. Discharged nickel oxide electrode contains mainly nickel hydroxide, $Ni(OH)_2$, while the high-charged phase is a n-type semiconductor and the discharged one is an electronic insulator or a low conductivity p-type semiconductor [12]. Hence the ohmic resistance of Ni–MH cell at low state of charge varies with state of charge. In Fig. 7, charge transfer resistance R_r increased with state of charge. The R_r value at 0% SOC was not plotted, since it was much higher than the values at other states of charge. Viswanathan et al. [3] found similar phenomenon for studies of state of charge in Cd–Ni cell. The increase in R_r with state of charge may be due to depletion of charged active material, leading to unavailability of active centers for charge transfer.

4. Conclusions

Through measurement of impedance spectrum at various states of charge, the changes of impedance modulus, $|Z|$, phase angle, ϕ, and equivalent series capacitance, C_s, with state of charge in Ni–MH cell have been studied. The experimental data were fitted with equivalent circuit containing CPE elements that represent double layer

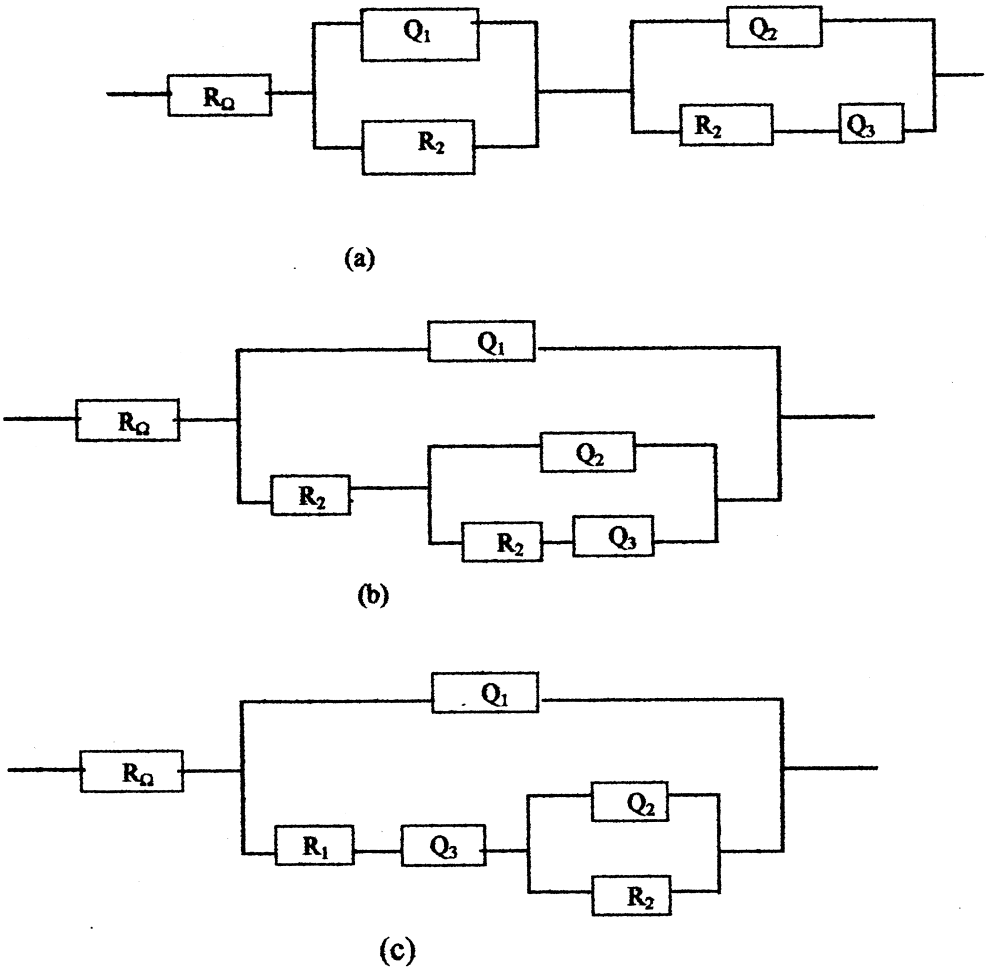

Fig. 4. Equivalent circuits adopted for MH/Ni cell at different state of charge.

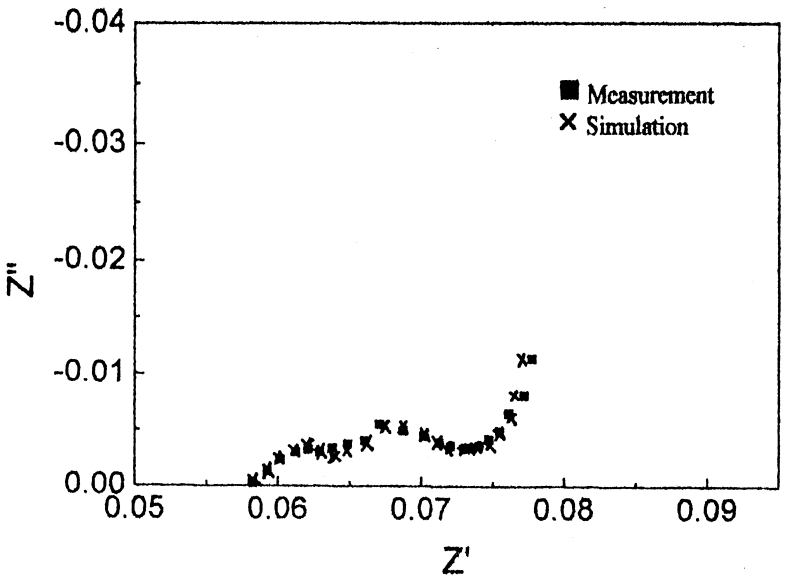

Fig. 5. Experimental and fitted impedance spectrum for MH/Ni cell at 80% state of charge.

Table 2
Equivalent circuit parameters for the circuit $R_{\Omega}(Q_1(R_1Q_3(Q_2R_2)))$

SOC/%	$R\Omega/\Omega$	Y_1	N_1	R_1	Y_3	N_3	R_2	Y_2	N_2
0	0.089	10.75	0.9	0.11	13	0.44			
20	0.077	0.296	1	0.0046	255	0.6	0.0248	9.79	0.6
40	0.063	10.6	0.65	0.0183	321	0.54	0.0763	10.63	0.62
60	0.061	0.786	1	0.0038	368	0.58	0.0178	12.8	0.64
80	0.059	97.9	0.78	0.0086	436	0.63	0.0138	11	0.79
100	0.058	3.14	0.65	0.0094	422	0.66	0.0135	9.99	0.84

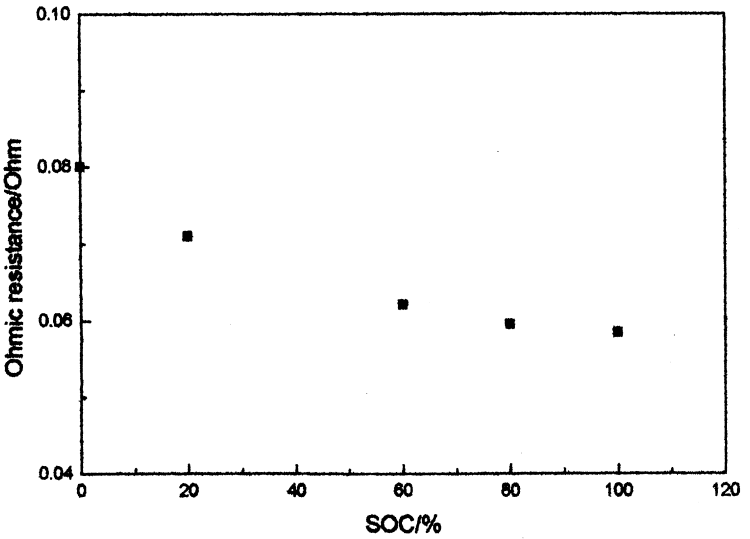

Fig. 6. Effect of state of charge on Ohmic resistance.

capacitance and Warburg resistance. The results showed that the equivalent circuit could satisfactorily fit experimental data. $|Z|$, ϕ and C_s were sensitive to SOC at low frequencies. The ohmic resistance decreased slightly with increase in SOC, but the magnitude of decrease is very small. The charge transfer resistance increased with state of charge. Therefore, it is concluded that a successful non-destructive monitoring of the state of charge of a Ni–MH cell is practically feasible by the measurement of ϕ and C_s at sufficiently low a.c. frequencies.

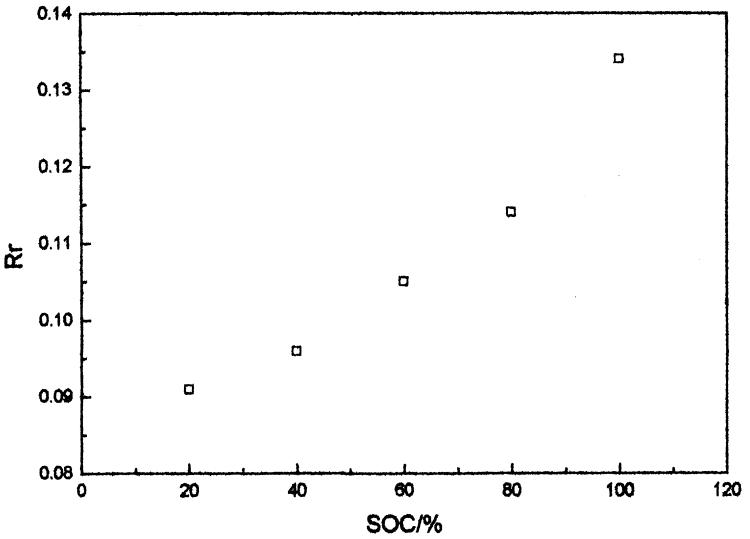

Fig. 7. Effect of state of charge on charge transfer resistance.

Acknowledgements

The authors are grateful for the financial support for this work by Postdoctoral Science Fund of China.

References

[1] K.A. Murugesamoorthi, S. Srinivasan, A.J. Appleby, J. Appl. Electrochem. 21 (1991) 95.
[2] W. Xianyou, Z. Yunshi, Y. Jie et al., Trans. Nonferrous Met. Soc. China, 8 (1998) 666.
[3] V.V. Viswanathan, A.J. Salkind, J.J. Kelley, J.B. Ockerman, J. Appl. Electrochem., 25 (1995) 716.
[4] R.T. Barton, M. Hughes, S.A.G. Karunathilaka, N.A. Hampson, J. Appl. Electrochem. 15 (1985) 399.
[5] M.S. Suresh, S. Sathyanaryana, J. Power Sources 37 (1992) 335.
[6] Ph. Blanchard, J. Appl. Electrochem. 22 (1992) 121.
[7] S. Sathyanaryana, S. Venugoplan, M.L. Gopikanth, J. Appl. Electrochem. 9 (1979) 125.
[8] B.A. Boukamp, Equivalent Circuit Users Manual, 2nd, University of Twente, The Netherlands(1989)
[9] M.S. Suresh, J. Power Sources 50 (1994) 375.
[10] M.A. Reid, J. Power Sources 47 (1994) 277.
[11] N. Kuriyama, T. Sakai, H. Miyamura et al., J. Electrochem. Soc., 139 (1992) L72.
[12] R. Barnard, G.T. Crickmore, J.A. Lee, F.L. Tye, J. Appl. Electrochem. 10 (1981) 61.